

Scanning Microscopy

Volume 1992
Number 6 *Signal and Image Processing in
Microscopy and Microanalysis*

Article 30

1992

Random Access Direct Parallel Detection of Electron Energy Loss Spectra with a New Photodiode Array

Stephan la Barré
Technische Universität Berlin, Germany

Eckhard Quandt
Technische Universität Berlin, Germany

Heinz Niedrig
Technische Universität Berlin, Germany

Follow this and additional works at: <https://digitalcommons.usu.edu/microscopy>



Part of the [Biology Commons](#)

Recommended Citation

la Barré, Stephan; Quandt, Eckhard; and Niedrig, Heinz (1992) "Random Access Direct Parallel Detection of Electron Energy Loss Spectra with a New Photodiode Array," *Scanning Microscopy*. Vol. 1992 : No. 6 , Article 30.

Available at: <https://digitalcommons.usu.edu/microscopy/vol1992/iss6/30>

This Article is brought to you for free and open access by the Western Dairy Center at DigitalCommons@USU. It has been accepted for inclusion in Scanning Microscopy by an authorized administrator of DigitalCommons@USU. For more information, please contact digitalcommons@usu.edu.



RANDOM ACCESS DIRECT PARALLEL DETECTION OF ELECTRON ENERGY LOSS SPECTRA WITH A NEW PHOTODIODE ARRAY

Stephan la Barré*, Eckhard Quandt, Heinz Niedrig

Optisches Institut, Technische Universität Berlin, Sekr. P11,
Straße des 17 Juni 135, 10623 Berlin, Germany

Abstract

A new type of photodiode array (PDA) which allows the individual access of single diodes is used to record energy loss electrons directly without electron photon conversion.

The detector is part of an electron energy loss parallel detection system which consists of a sector field spectrometer and a quadrupole lens system to magnify the spectra electron-optically.

The parallel detector is a new random access PDA (RAPDA) which allows the individual access of single diodes. Therefore, different parts of the spectrum with dramatically different electron rates (zero loss peak, plasmon loss, ionization edges) can be recorded, each with optimum acquisition time and number of read-outs. This method allows the use of all available information in one recording of a spectrum for an increased intensity range compared to self-scanning PDAs (SSPDAs) where all the diodes have to be read out in a row.

Direct illumination of the diodes increases the sensitivity of the detector by two orders of magnitude for 40 keV electrons compared to detectors with electron photon conversion. No apparent radiation damage of the diodes was observed if the detector was cooled down to temperatures below -80°C .

Key Words: Electron energy loss spectroscopy (EELS), parallel EELS, parallel detector, photodiode array, direct electron detection.

*Address for correspondence:

Stephan la Barré
Optisches Institut,
Technische Universität Berlin, Sekr. P11,
Straße des 17 Juni 135,
10623 Berlin, Germany

Telephone number: 49-(030)-314 25 023

FAX number: 49-(030)-314 26 888

Introduction

In this paper, we outline a direct parallel detection system that has been developed to record low intensity electron energy loss spectra (EELS). Parallel detection shows superior overall performance compared to serial detection. This extends the range of application for EELS in analytical science. Parallel detection dramatically reduces acquisition time by a factor of about 1000 allowing EELS recording of radiation sensitive materials or the measurement of high loss spectra with low statistical error⁸.

Commercial semiconductor arrays like charge-coupled devices (CCDs) or photodiode arrays (PDAs) are used as parallel detectors for EELS. In the direct mode, these arrays are directly irradiated by electrons. Compared to indirect registration, where electrons are scintillated before detection, the direct method provides a higher sensitivity and therefore a superior behavior for the detection of low electron rates.

In the past, only self-scanning PDAs (SSPDAs) had been available. Due to the shift-register architecture all diodes of the array have to be read out in a row. This read-out procedure limits the minimum read-out time and therefore the detectable intensity range of the detector. An improvement can be obtained by a new random access PDAs (RAPDAs) which allow the access of individual diodes. Therefore, different parts of the spectrum with dramatically different electron fluxes (zero loss peak, plasmon loss, ionization edges) can be recorded, each with optimum acquisition time and number of read-outs. This method allows the use of all available information in one recording of a spectrum for an increased intensity range. Due to the increased complexity of the read-out process and the high data rates, EELS acquisition with a RAPDA requires more sophisticated computer control and data processing capabilities compared to SSPDAs.

Parallel EELS Instrumentation

The parallel EELS detection (PEELS) device consists of a double-focusing magnetic sector field spectrometer¹, post-spectrometer magnification optics and a parallel detector. Figure 1 shows the schematic diagram

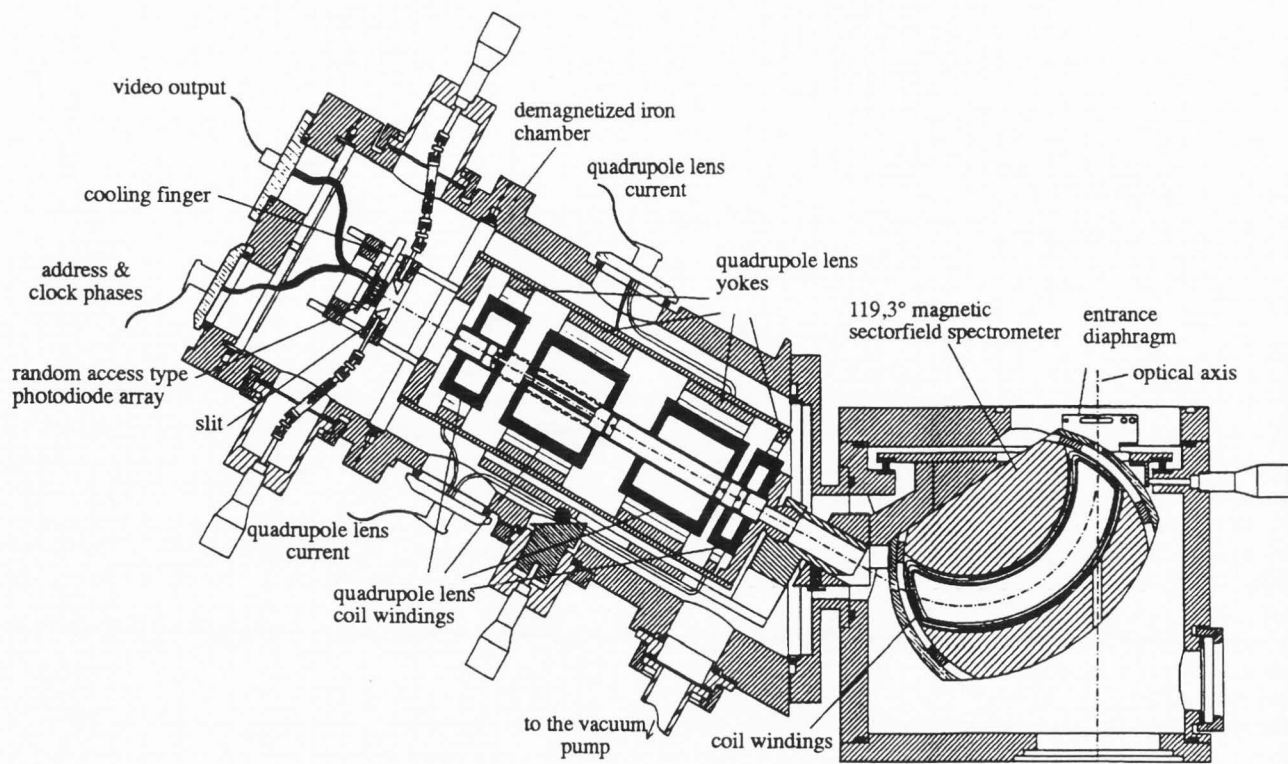


Figure 1. Schematic diagram of the double focussing sector field spectrometer combined with the quadrupole lens system and the parallel detector in the vacuum chamber of the scanning transmission electron microscope.

Table 1. Performance characteristics of the energy analyzer.

Spectrometer	
Maximum aperture	40 mrad
Deflection angle	119.3°
Deflection radius	70 mm
Dispersion at 40 keV	3.5 $\mu\text{m}/\text{eV}$
Quadrupole lens system	
Number of lenses	4
Magnification	4 ... 86
System length	225 mm
Primary electron energy	20 ... 80 keV
Energy resolution at 40 keV	1.1 eV

of the instrument; its three parts are completely placed in the magnetic shielded vacuum chamber. The performance characteristics of the energy analyzer are summarized in Table 1.

The EEL-spectrometer can be used for primary energies from 20 to 80 keV. For 40 keV, the sector field provides a dispersion of 3.5 $\mu\text{m}/\text{eV}$. Since CCDs or PDAs typically have an element spacing of approximately 25 μm , the spectrum has to be magnified to obtain a satisfactory energy resolution in the case of parallel detection. If we consider direct electron registration then the post-spectrometer magnification has to operate

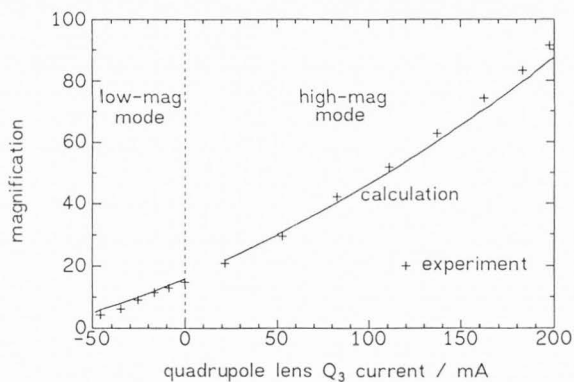


Figure 2. Experimental and calculated magnification of the QLS versus the current of the final lens Q_3 for the low- and high-magnification mode.

electron-optically. For that purpose, a quadruplet was built according to a design by Scott⁹. The system provides a variable magnification of the dispersive direction ranging from 4 to 86 (Fig. 2). All lenses are placed behind the spectrometer. The quadruplet uses the dispersion plane as a real object, such that the optical properties of the spectrometer are not affected. Quadrupole lenses have a number of advantages compared to round magnetic lenses: no image rotation, cylinder-optical imaging, and lower power consumption. Additionally, the

system is designed with magnification-independent cross-overs, so that fixed slits can be attached to minimize stray scattering⁹.

The detector is placed in the image plane of the quadrupole lens system (QLS) and can be adjusted in the non-dispersive direction from outside the vacuum chamber. To use the PDA as a direct parallel detector, the quartz-glass window was removed. To protect the shift-register circuitry, as well as the edge region of the photodiodes against electron irradiation, a platinum mask is placed directly above the array.

This universal EEL-spectrometer (the sector field in combination with the magnification system) allows the recording of the spectra in two different ways.

Direct-indirect detection of electrons

In the direct mode, the electrons directly irradiate the parallel detector. They generate electron-hole-pairs (EHPs) with a mean generation energy of 3.64 eV provided that the energy is absorbed in or near the depletion layer of the p-n-junction. Considering a SiO₂-passivating layer, and the depth profile of the diodes, the energy dependence of the EHP generation rate (Fig. 3) can be explained. Low energy electrons are mainly absorbed in the passivating layer and do not contribute to the discharge of the diode. At the high end of the energy scale, an increasing fraction of the electron energy is absorbed in deeper regions of the substrate where most of the generated charge recombines and does not contribute to the discharge process. Nevertheless, the rate for 40 keV electrons is about two orders of magnitudes higher compared to values obtained in the common indirect mode⁶. In the indirect mode, the electrons are converted to photons by a scintillator (yttrium-aluminum-garnet, YAG single crystal) which is usually fiber-optically coupled to the parallel detector. In order to compare the two detector types, we define the EHP generation rate, η , as the number of generated EHPs in the diode per incident electron for both detector types. In the case of the indirect detector, there are losses due to electron-photon conversion efficiency, light spread in the scintillator, and reflection and transfer losses through the fiber-optical coupling. All these losses are included in η . The high value of η for the direct detector influences the main detector characteristics, e.g., the detection quantum efficiency (DQE) which is a measure of the quality of an electron detector and represents a value which describes the noise performance of the detector. The DQE is best defined as:

$$\text{DQE} = (\text{SNR}_{\text{output}} / \text{SNR}_{\text{input}})^2 \quad (1)$$

where $\text{SNR}_{\text{input}}$ and $\text{SNR}_{\text{output}}$ are the signal-to-noise (SNR) ratios at the input and output of the detector.

Radiation damage

The radiation damage is a general disadvantage of the direct mode which leads to an irreversible increase of the dark current⁵. This damage depends dramatically on the temperature of the detector. No apparent damage

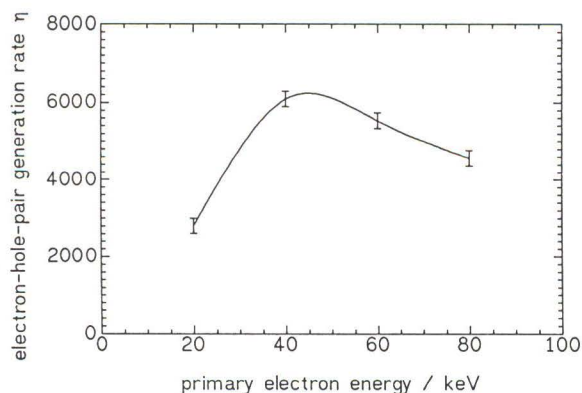


Figure 3. Electron-hole pair generation rate as a function of electron energy.

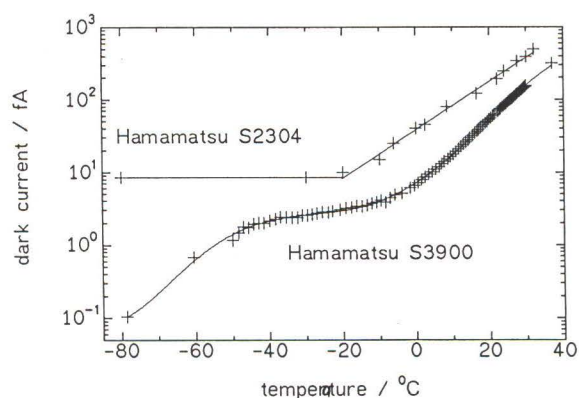


Figure 4. Dark current versus temperature for two different PDAs.

was observed if the detector was cooled down to temperatures below -80°C ⁷. As a side effect, the dark current is further reduced (Fig. 4) compared to the recommended operating temperature of -20°C . To obtain the required temperatures, the parallel detector is mounted on a liquid nitrogen cooled stage in the vacuum.

Noise

If all noise due to beam intensity fluctuations and other instrumental effects is ignored, the $\text{SNR}_{\text{input}}$ is equal to the shot noise σ'_s of the incident electron beam³. If N_i is the number of electrons incident on a single detector element, then we can write:

$$\sigma'_s = N_i^{1/2} \quad (2)$$

To define the $\text{SNR}_{\text{output}}$, it is necessary to add several noise sources of the array and the signal electronics. The following noise terms are all given in units of EHPs generated in a single detector element.

The shot noise (σ_s) of the primary beam in terms of generated EHPs is:

$$\sigma_s = \eta N_i^{1/2} \quad (3)$$

The dark current d_c of the diodes might become a problem in experiments with low count rates and long

integration time. The effective dynamic range of the diode is decreased because the charge generated by the dark current saturates the diodes. The noise of the dark current (σ_c) is:

$$\sigma_c = (d_c \cdot t)^{1/2} \quad (4)$$

where t is the dwell time in seconds and d_c the dark current rate (electrons in the PDA per second).

There is another type of noise from the dark current that becomes obvious in measurements with long integration time. The dark current rates of the individual diodes show a slight variation. This effect of root-mean-square (rms) fractional dark-current rate variation leads to the following noise term:

$$\sigma_{c\nu} = \nu_d \cdot d_c \cdot t \quad (5)$$

where ν_d is a measure for the short range channel-to-channel rate variation. The ν_d value, which has been taken for the calculations of the SNR and the DQE, is of the order of 0.5%⁴. Superimposed as a fixed pattern noise on the spectrum is the rms fractional gain variation ν [channel-to-channel gain variations (ctc)] between adjacent diodes of the array which give rise to a noise component σ_ν which is proportional to the number of accumulated electrons in the PDA.

$$\sigma_\nu = \nu \eta N_i \quad (6)$$

Additionally, the read-out of a single detector element is associated with electronic noise σ_e which is due to reset noise of the video line, noise present on the circuit grounds and supply voltages, amplifier noise, and noise due to analog-to-digital (A/D) conversion (ADC) of the diode signal.

Signal-to-noise (SNR) ratio and detection quantum efficiency (DQE)

Combining the noise terms mentioned above, the SNR at the input and output of the detector is

$$\text{SNR}_{\text{input}} = N_i / (N_i)^{1/2} = N_i^{1/2} \quad (7)$$

$$\text{SNR}_{\text{output}} = N_i / [N_i + (\sigma_c^2 + \sigma_{c\nu}^2 + \sigma_e^2 + \sigma_\nu^2) / \eta^2]^{1/2} \quad (8)$$

$$\text{SNR}_{\text{output}} = N_i^{1/2} [1 + (\eta^2 N_i)^{-1} \times \{(d_c t)^2 + (\nu_d d_c t)^2 + \sigma_e^2 + (\eta \nu N_i)^2\}]^{-1/2} \quad (9)$$

To calculate the DQE, we can use equations (1), (7) and (9), and with $N_i = st$, where s is the rate of incident electrons and t is the dwell time, we get the expression:

$$\text{DQE} = [1 + \eta^{-2} \{d_c/s + (\nu_d^2 d_c^2 t)/s + \sigma_e^2/st\} + st\nu^2]^{-1} \quad (10)$$

Accumulation of multiple read-outs

Equations (8) and (10) apply to data recorded in a single read-out defined by the rate of electrons incident on the detector during a dwell time t , resulting in a total number of recorded electrons N_i . The given exposure

time can be divided into m periods and the m separate read-outs have to be added electronically. The decrease of dwell time by a factor $1/m$ leads to an increase of the maximum electron rate which can be recorded by the detector without being saturated. The diode shot noise depends on the total exposure time, and is therefore, the same as for a single read-out². The accumulated read-out noise and the A/D-conversion noise are both increased since these noise terms will be added randomly in every read-out. This gives a new expression for the $\text{SNR}_{\text{output}}$:

$$\text{SNR}_{\text{output}} = N_i / [N_i + (\sigma_c^2 + \sigma_{c\nu}^2 + m\sigma_e^2 + \sigma_\nu^2) / \eta^2]^{1/2} \quad (11)$$

The SNR at the output of the detector is plotted in Figure 5. In the low dose region, the $\text{SNR}_{\text{output}}$ of the direct detector is higher than in the indirect mode since the direct η value is about 2 orders of magnitude higher than the indirect value. Above $2 \cdot 10^4$ recorded electrons, the diodes of the direct detector saturate at a maximum SNR of about 100. In the region between $2 \cdot 10^4$ and $2 \cdot 10^6$ incident electrons, only the indirect detector is working with a SNR which is 1000 at maximum. Additionally, Figure 5 shows examples of the $\text{SNR}_{\text{output}}$ for different multiple read-out numbers (m) independent of the overall dwell time.

The noise and the minimal detectable signal increase in the multiple read-out case. On the other hand, the maximum output signal which corresponds to the complete discharge of the diode increases by a factor m because the charge of each diode is reset after every read-out.

To get an expression for the DQE in the multiple read-out case we have to combine equations (11) and (10):

$$\text{DQE} = [1 + \eta^{-2} \{d_c/s + (\nu_d^2 d_c^2 t)/s + m\sigma_e^2/st\} + st\nu^2]^{-1} \quad (12)$$

Figure 6 shows the calculation of the DQE as a function of the incident electron number per diode for direct and indirect electron registration. The data indicates a better performance of direct mode up to $2 \cdot 10^4$ incident electrons for the higher EHP generation rate. Above $2 \cdot 10^4$ electrons per channel, the diodes saturate only in the direct detector. For indirect detection, the saturation limit is two orders of magnitude higher. The DQE dependence for different multiple read-out numbers (m) and overall integration time values is also shown. The add-up of read-out noise for each read-out procedure let the DQE decrease in both detection modes. The values for the above stated noise terms are taken from Table 2. It should be noted that the value of 0.25% for the channel-to-channel gain variation is a property of the diode array hardware. This can be reduced by dividing the recorded spectrum with a reference spectrum showing the variation of the detector gain or by other methods which need to acquire energy shifted spectra in rapid succession (first-, second-, or higher order difference

Direct parallel detection of EELS

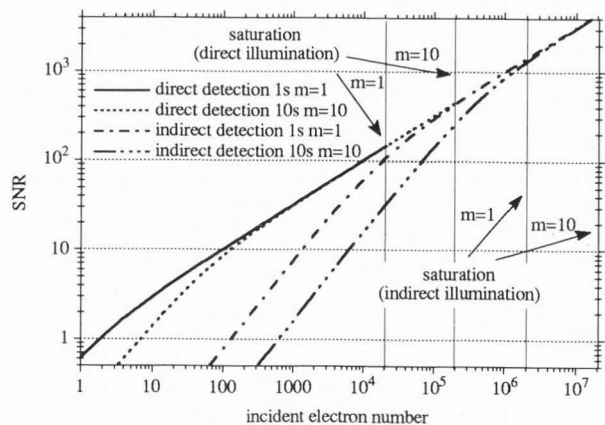


Figure 5. SNR at the output of the diode array for the direct ($\eta = 6000$) and indirect detection mode ($\eta = 62$), both with 1 second dwell time in a single read-out $m = 1$ and with an overall dwell time of 10 seconds for $m = 10$ read-outs. Channel-to-channel gain variations of 0.25% has been used in the calculations.

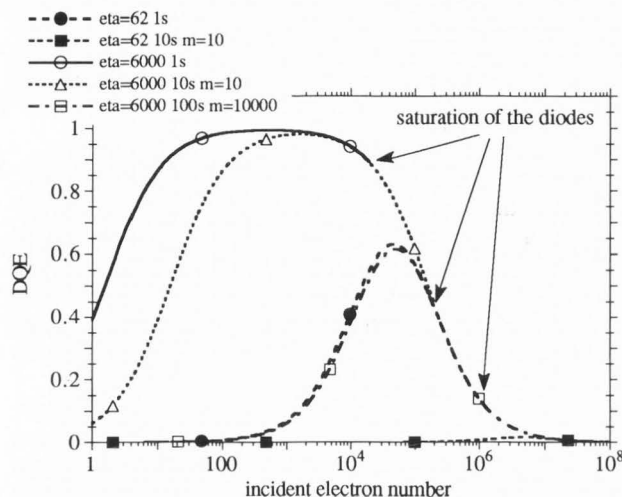


Figure 6. Detection quantum efficiency (DQE) as a function of the number of incident electrons for the direct mode $\eta = 6000$ (marked with $\eta = 6000$) and indirect mode with $\eta = 62$ (marked with $\eta = 62$) for different overall integration times (1, 10, and 100 seconds) and number of read-outs. Channel-to-channel gain variations of 0.25% has been used in the calculations.

spectrum)⁶. A lower value of channel-to-channel gain variation would cause an improvement of the DQE for both detector types.

Random access photodiode array (RAPDA)

The RAPDA Hamamatsu S3900-X is a new type of detector that operates like direct-memory-access devices. It allows to read out diodes or groups of diodes individually instead of reading out all the diodes in a row, as is necessary for PDAs with self-scanning shift-registers. The random access operation offers many new

Table 2. Performance characteristics of a SSPDA and a new RAPDA.

Photodiode array type	SSPDA S2304	RAPDA S3900
Number of elements	512	512
Element spacing	25 μm	25 μm
Active area	13x2500 μm^2	13x2500 μm^2
Depth SiO ₂ passivating layer	0.4 μm	1.0 μm
Doping of active area	p	n
Depth of active area	1.2 μm	1.0 μm
Capacity	2 pF	10 pF
Bias voltage	5 V	2 V - 7 V
Saturation charge	10 pC	20 pC - 70 pC
Dark current at 20 °C (-80 °C)	10 fA (8.5 fA)	2 fA (0.1 fA)
Noise (equivalent charge)	2250 e ⁻	2250 e ⁻
Minimal integration time for N diodes	10 ms (N=512)	10 ms (N=512) t=N*16 μs
Max. current/diode (40 keV e ⁻)	160 fA	16 pA - 58 pA
Non-uniformity of response	0.3%	0.3%

measuring possibilities and improves the performance of a PDA as a parallel detector for EELS, as discussed below.

The pixel size of the RAPDA is unchanged compared to the SSPDAs, while the thickness of the passivating-layer is increased and the depletion-layer is decreased along with a doping exchange of the p-n-junction. The changes result in an increase of capacity (by a factor of 5) to 10 pF. In the recommended mode, however, the important saturation charge is increased by a factor of only two due to the lower bias voltage of 2 V, compared to 5 V in the case of the SSPDA. The consequence of the higher saturation charge is an increase of the dynamic range by the same factor. A further rise to a factor of 7 can be achieved by higher bias voltage in combination with higher amplitudes of the clock phases. Parameters for a current generation RAPDA S3900-512 and of an older device SSPDA S2304-512 are given in Table 2.

For a RAPDA with 512 diodes, an address of 10 bit (only 9 bit are used) has to be provided together with a certain digital pattern of the 3 clock phases to choose a particular diode and to connect it to the video-line. Another important property of the detector, the minimum read-out time, is limited by the maximum read-out frequency and, in the case of the RAPDA, additionally by the recorded number of diodes. Using the Hamamatsu driver/amplifier circuit C4072, the maximum frequency (62.5 kHz) is unchanged such that the read-out time for all diodes is approximately the same as for the SSPDA. According to Hamamatsu, this frequency can be increased to 1 MHz for the RAPDA, which requires sophisticated analog electronics instead of the C4072 circuit. Even for the same read-out

frequency, the minimum read-out time of the RAPDA can be decreased compared to the SSPDA, provided that only parts of the array are read out. The decreasing factor is approximately given by the number of selected diodes divided by 512. Because high intensity parts of EELS (for example, the primary peak) are often only spread over a few diodes [for a magnification of 40x the primary peak with $\Delta E = 1.1$ eV and a spectrometer dispersion of $3.5 \mu\text{m}/\text{eV}$ (40 keV electrons) corresponds to a full-width-half-maximum (FWHM) of less than 7 diodes], a reduction factor of about 40 should be reachable in practice.

The feature to set the measuring time for each diode or group of diodes individually offers the possibility to record EELS with an optimum collecting time for each part of the spectrum. While the diodes still collect charge in low intensity regions, the diodes in high intensity parts can be read out several times. The number of equal spectrum parts are stored and can be further processed and analyzed. To get the same information with a SSPDA, the different parts of the spectrum have to be scanned one after another choosing a suitable recording time for each part. Compared to a RAPDA this means a higher over-all measuring time and subsequently higher irradiation damage of the target. Additionally, the information recorded with a SSPDA would not be truly detected in parallel.

To illustrate the advantages of the RAPDA in direct and indirect modes, Figure 7 shows the DQE as a function of the incident electron rate for different dwell times. The minimum value of the integration time τ_{min} for the SSPDA is 10 ms whereas τ_{min} for the RAPDA is set to $512 \mu\text{s}$ which corresponds to a read-out time of 32 diodes. It can be seen that the DQE in the direct mode is very close to unity over a wide range of incident electron rates. The upper detection limit for a high incident electron rate is determined by saturation effects of the diodes and the minimum integration time, τ_{min} . It is clear that the DQE of an SSPDA would degrade earlier due to the higher minimum integration time.

Data Acquisition

Data acquisition with a RAPDA requires computer control to manage the complex timing process with a reasonable time resolution. Additionally, the generated data has to be interfaced, digitized, and stored for image processing and analysis.

The hardware of the data acquisition system is based on an Apple Macintosh IICI (68030 CPU, 25 MHz, 4 MB RAM) in combination with a Hamamatsu driver/amplifier board C4072, a data acquisition board Data-translation DT2227 (16 bit A/D resolution, 100 kHz throughput) and a self-developed timer board.

The data acquisition software was written in C following Apple's user interface guidelines which let the operator simply choose the experimental parameters and provides tools for image processing.

The RAPDA has to be provided with the 10 bit address and the clock signals. All of these signals are

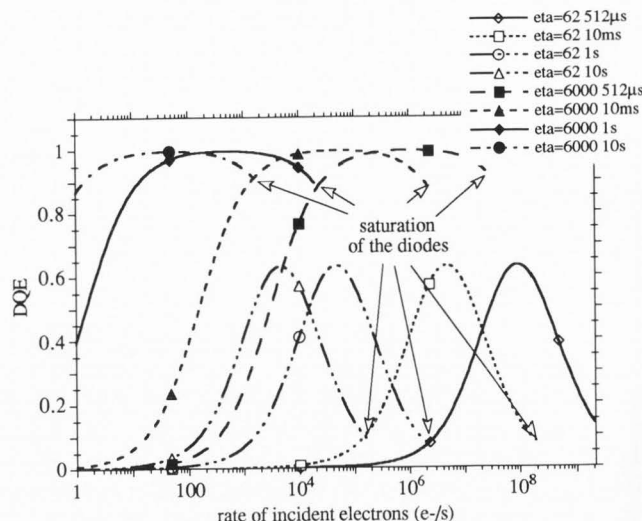


Figure 7. Detection quantum efficiency (DQE) as a function of the incident electron rate for the direct mode $\eta = 6000$ (marked with $\eta=6000$) and indirect mode with $\eta = 62$ (marked with $\eta=62$) in a single read-out for different overall dwell times using a RAPDA. The different saturation-rate values depend on the dwell time and are marked by arrows.

generated on the external timer board to achieve a reasonable time resolution on a nanosecond time scale. Current integration, amplification, and noise filtering of the RAPDA output signal are done on the C4072 board. The output signal of the C4072 is directly connected to the ADC of the Data-translation board. After digitizing, the data are written to an on-board 512 kB memory or directly into the RAM of the computer (Fig. 8).

To simplify the development of the timer hardware, a maximum of 4 different diode groups with fixed integration time ratios of 1, 10, 100, and 1000 are allowed. The first and the last diode for each group of the four have to be chosen along with a minimum integration time. All values are transmitted to the timer board through the two 8 bit digital input/output (I/O) ports of the DT2227. A further pulse starts the timer that generates the addresses and clock signals corresponding to the transmitted information. At the same time, the RAPDA output data, for example, the different number of scans for each group of diodes, are digitized, summed, and stored. After the whole scan is recorded, the spectrum is displayed and further processing can take place.

Conclusions

In this paper we described the performance of a new RAPDA for the use as a parallel detector in EELS. When used in the direct mode, the RAPDA provides high sensitivity and therefore a superior behavior for the detection of low electron fluxes compared to the indirect mode.

It has been shown that the radiation damage is no longer a severe problem when the array is cooled with

Direct parallel detection of EELS

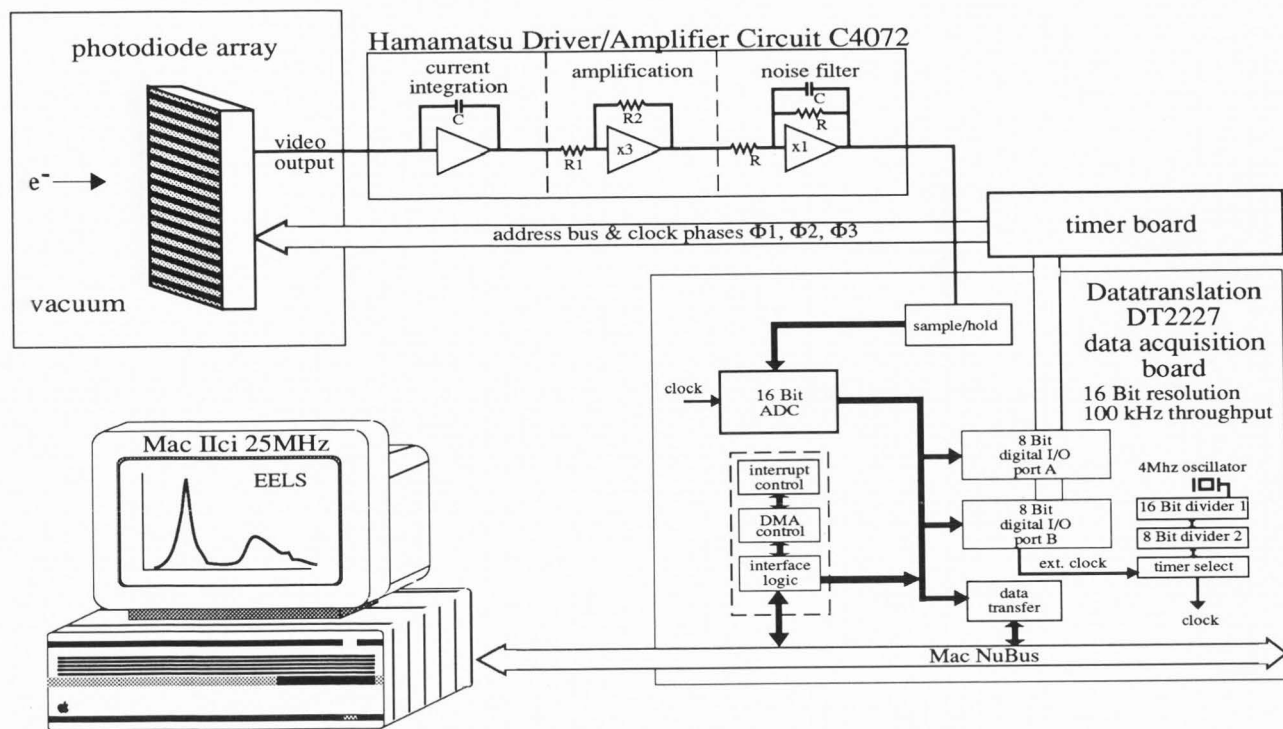


Figure 8. Block diagram of the data acquisition hardware.

liquid nitrogen; in addition the dark current is dramatically reduced.

With the RAPDA, it is possible to improve upon a fundamental disadvantage of the direct mode (i.e., the measurement of high intensities when only a small number of diodes is concerned). Furthermore, different parts of an EELS can be measured with individual integration times such that the DQE is maximum. To improve the statistical error, multiple read-outs of high and medium intensity parts of the spectrum are possible simultaneously with the acquisition of the low intensity (high integration time) regions.

Acknowledgment

The authors are grateful to Apple Computer GmbH Germany for the loan of the computer system.

References

1. Crewe AV, Isaacson M, Johnson D (1971) A high resolution electron spectrometer for use in transmission scanning electron microscopy. *Rev. Sci. Instr.* **42**, 411-419.
2. Egerton RF (1986) *Electron Energy Loss Spectroscopy in the Electron Microscope*. New York 1986. Plenum Press, NY. pp. 106-111.
3. Egerton RF, Yang YY, Cheng SC (1993) Characterization and use of the Gatan 666 parallel-recording electron energy-loss spectrometer. *Ultramicrosc.* **48**, 239-250.

4. Jonas P, Schattschneider P (1991) Electron Compton scattering with parallel detection: an experiment with very low count rates. *Ultramicrosc.* **38**, 117-126.

5. Jones BL, Jenkins DG, Booker GR, Fry PW (1977) Use of silicon linear arrays for detection of high-energy electrons. *Inst. Phys. Conf. Ser.* **36**. Bristol, U.K., 73-76.

6. Krivanek OL, Ahn CC, Keeney RB (1987) Parallel detection electron spectrometer using quadrupole lenses. *Ultramicrosc.* **22**, 103-115.

7. Quandt E, la Barré S, Hartmann A, Niedrig H (1990) Parallel detection of electron energy loss spectra in direct mode. In: *Microbeam Analysis 1990*. San Francisco Press. 43-47.

8. Quandt E, la Barré S, Niedrig H (1990) Direct parallel detection of energy resolved large angle convergent beam patterns. *Ultramicrosc.* **33**, 15-21.

9. Scott CP (1988) A quadrupole lens system for use in the recording of electron energy loss spectroscopy. Ph.D. Thesis, University of Glasgow, U.K.

Discussion with Reviewers

P. Schattschneider: Is the described system good for 200 keV also? If so, what would be the conversion rate in that case, and would you expect more radiation damage?

Authors: We do not have experimental results for higher primary beam voltages than 80 keV. We think that the conversion rate will decrease further because most of the electron energy will be deposited deep in the

substrate of the array and not in the depletion zone of the p-n-junction. It could be advantageous to use a thicker SiO₂ layer so that the area of maximum energy deposition will lie in the depletion area of the diode.

P. Schattschneider: Can you estimate the lifetime of your PDAs at -80°C?

Authors: The estimate of the lifetime is difficult because in 8 months, we have not seen any degradation at this temperature. Destruction tests by applying very high intensities, that are not common in EELS, would be necessary to answer your question. Unfortunately we cannot afford to do such experiments and destroy the arrays by purpose.

During one experiment the address-register of the RAPDA, which is usually masked, was directly irradiated with 40 keV electrons. Thereafter, the read-out of the diodes was no longer possible which shows that the shift-register electronics is very sensitive to direct electron irradiation.

P. Schattschneider: What about thermal movements of the array or its mount during cool-down?

Authors: Movement of the array position during cool-down has not been observed. However, the detector and QLS can be adjusted individually to cope with alignment errors in our experimental setup.

P. Schattschneider: Can you explain why the dark current is so different for the two arrays, and why it is almost independent of the temperature for the self-scanned array?

Authors: The two arrays have different junction design and shift-register architecture. The SSPDA S2304-512 scanning circuit is constructed by a plasma-coupled-device (PCD) and a switching section using p-n-p-transistors. The PCD image sensor dark output is caused both by photodiode dark current and by PCD shift register leakage current. The effect of photodiode leakage current is dominant in the high temperature region. The shift-register leakage current, including the p-n-p-transistor bias current, seems to remain almost constant, giving a fixed offset, even at very low temperatures where the dark current is small.

The RAPDA S3900-512 is manufactured by applying n-type metal-oxide semiconductor (NMOS) technology. The p-n-p-transistor switch is replaced by a MOS transistor which probably causes a lower shift-register leakage current. We think that the decrease of leakage current below -40°C is due to the new shift-register construction which probably also has a temperature dependent leakage current.

P. Schattschneider: Is there a dead time during the read-out of selected diodes?

Authors: No.

A.J. Bourdillon: In this spectrometer, do you observe background signal due to stray electrons? Can you normally record spectra with energy losses greater than 2 keV?

Authors: We have not measured any loss greater than a few hundred eV. The QLS is designed with magnifica-

tion-independent crossovers, so that fixed slits can be attached to minimize stray scattering. We included slits according to the suggestions of C.P. Scott⁹.

O.L. Krivanek: Directly-illuminated PDAs saturate at an incident electron dose per channel of about 10⁴ 40 keV electrons (S2304), and 2 · 10⁴ electrons (S3900). In order to get the 10⁸ counts necessary for reducing the statistical noise in a spectrum to 0.01% (a level that several PEELS laboratories are attaining these days) more than 10,000 spectra will therefore have to be read out and added up. In view of this, would the authors recommend the directly illuminated PDA for work aiming to improve the detection limits of EELS beyond those attainable by energy dispersive X-ray spectroscopy through the acquisition of exceptionally noise free spectra? If their answer is yes, how much radiation damage in the PDA would they expect after a few days of acquiring spectra at these intensities?

Authors: At an incident dose of 10⁴ electrons per diode and an acquisition time of 10 ms for the read-out of the whole array, an overall measuring time of 100 seconds will be necessary and can further be reduced when a higher scan frequency of the array is applied; 10⁴ spectra have to be read out. The radiation damage of the probe will not be a problem because the total dose for both detection modes is about the same. The accumulation of read-out noise is a serious problem because the adding-up of 10⁴ spectra will increase the noise by a factor of 100 (noise for m read-outs is m^{1/2} times the noise of a single read-out). With direct illumination, the increase of noise caused by the adding-up of multiple read-outs is partly compensated by the difference of the EHP-generation rate between direct and indirect detection that is of the order of 100. The question of radiation damage caused by fast electrons can only be answered for 40 keV electrons. We used a SSPDA in direct mode for several months with different intensities and could not observe any changes in the characteristics of the diode response. Especially the dark current did not increase when the array was cooled below -80°C.

R.F. Egerton: Do you see any non-linearity in the intensity response, as has been reported for indirect-exposure photodiode-array systems?

Authors: If we used intensities which are detectable with the direct detector, we have not observed any non-linearities.

R.F. Egerton: What is the current status of the project? Do you hope to market or make available the hardware or software?

Authors: We are not planning to market the hardware or the software. The whole system was built to record energy-resolved large angle convergent beam patterns in the rocking crystal method with a scattering vector of $q = g/2$ (g , reciprocal lattice vector). That means low intensity spectra and therefore very long integration times. To cope with radiation damage of the crystal and long range instabilities of the microscope, we needed a sensitive detector. We believe that the direct detector is suitable for such an experiment.